AIRLOADS AND WAKE GEOMETRY CALCULATIONS FOR AN ISOLATED TILTROTOR MODEL IN A WIND TUNNEL

Wayne Johnson

Army/NASA Rotorcraft Division
NASA Ames Research Center
Moffett Field, California

Comparisons of measured and calculated aerodynamic behavior of a tiltrotor model are presented. The test of the Tilt Rotor Aeroacoustic Model (TRAM) with a single, 0.25-scale V-22 rotor in the German-Dutch Wind Tunnel (DNW) provides an extensive set of aeroacoustic, performance, and structural loads data. The calculations were performed using the rotorcraft comprehensive analysis CAMRAD II. Presented are comparisons of measured and calculated performance for hover and helicopter mode operation, and airloads for helicopter mode. Calculated induced power, profile power, and wake geometry provide additional information about the aerodynamic behavior. An aerodynamic and wake model and calculation procedure that reflects the unique geometry and phenomena of tiltrotors has been developed. There are major differences between this model and the corresponding aerodynamic and wake model that has been established for helicopter rotors. In general, good correlation between measured and calculated performance and airloads behavior has been shown. Two aspects of the analysis that clearly need improvement are the stall delay model and the trailed vortex formation model.

Notation[·]

a	speed of sound
A	rotor disk area, πR^2
c_n	blade section normal force coefficient, $N/(\frac{1}{2}\rho U^2 c)$
c_{ref}	blade reference chord
C_P	rotor power coefficient, $P/\rho(\Omega R)^3 A = Q/\rho(\Omega R)^2 RA$
C_T	rotor thrust coefficient, $T/\rho(\Omega R)^2 A$ (shaft axes)
C_X	rotor propulsive force coefficient, $X/\rho(\Omega R)^2 A$ (wind axes, positive forward)
$M^2 c_n$	blade section normal force coefficient times Mach number squared, $N/(\frac{1}{2}\rho a^2 c)$
M_{tip}	blade tip Mach number, $\Omega R/a$
N	number of blades
N	blade section normal force
r	blade radial station (0 to R)
R	blade radius
P	rotor power, $P = \Omega Q$

Q	rotor torque
T	rotor thrust (shaft axes)
U	blade section resultant velocity
X	rotor propulsive force (wind axes, positive forward)
α, α_s	rotor shaft angle (positive aft, zero for helicopter mode)
μ	advance ratio, $V/\Omega R$
ρ	air density
σ	rotor solidity, $Nc_{ref}/\pi R$
ψ	blade azimuth angle (zero azimuth is downstream)
Ω	rotor rotational speed

Introduction

The tiltrotor aircraft configuration has the potential to revolutionize air transportation by providing an economical combination of vertical take-off and landing capability with efficient, high-speed cruise flight. To achieve this potential it is necessary to have validated analytical tools that will support future tiltrotor aircraft development. These analytical tools must calculate tiltrotor aeromechanical behavior, including performance, structural loads, vibration, and aeroelastic stability, with an accuracy established by correlation with measured tiltrotor data. For many years such

		Form Approved *OMB No. 0704-0188*
Report Documentation Page	

<table>
<tr><td colspan="3">Public reporting burden for the collection of information is estimated to average 1 hour per response, including the time for reviewing instructions, searching existing data sources, gathering and maintaining the data needed, and completing and reviewing the collection of information. Send comments regarding this burden estimate or any other aspect of this collection of information, including suggestions for reducing this burden, to Washington Headquarters Services, Directorate for Information Operations and Reports, 1215 Jefferson Davis Highway, Suite 1204, Arlington VA 22202-4302. Respondents should be aware that notwithstanding any other provision of law, no person shall be subject to a penalty for failing to comply with a collection of information if it does not display a currently valid OMB control number.</td></tr>
</table>

1. REPORT DATE **2001**	2. REPORT TYPE	3. DATES COVERED **00-00-2001 to 00-00-2001**

4. TITLE AND SUBTITLE **Airloads and Wake Geometry Calculations for an Isolated Tiltrotor Model in a Wind Tunnel**	5a. CONTRACT NUMBER
	5b. GRANT NUMBER
	5c. PROGRAM ELEMENT NUMBER
6. AUTHOR(S)	5d. PROJECT NUMBER
	5e. TASK NUMBER
	5f. WORK UNIT NUMBER

7. PERFORMING ORGANIZATION NAME(S) AND ADDRESS(ES) **Army/NASA Rotorcraft Division,Army Aviation and Missile Command,Aeroflightdynamics Directorate (AMRDEC), Ames Research Center,Moffett Field,CA,94035**	8. PERFORMING ORGANIZATION REPORT NUMBER

9. SPONSORING/MONITORING AGENCY NAME(S) AND ADDRESS(ES)	10. SPONSOR/MONITOR'S ACRONYM(S)
	11. SPONSOR/MONITOR'S REPORT NUMBER(S)

12. DISTRIBUTION/AVAILABILITY STATEMENT **Approved for public release; distribution unlimited**

13. SUPPLEMENTARY NOTES **Presented at the 27th European Rotorcraft Forum, Moscow, Russia, September 11-14, 2001**

14. ABSTRACT

15. SUBJECT TERMS

16. SECURITY CLASSIFICATION OF:			17. LIMITATION OF ABSTRACT	18. NUMBER OF PAGES	19a. NAME OF RESPONSIBLE PERSON
a. REPORT **unclassified**	b. ABSTRACT **unclassified**	c. THIS PAGE **unclassified**	**Same as Report (SAR)**	**12**	

Standard Form 298 (Rev. 8-98)
Prescribed by ANSI Std Z39-18

correlation has been performed for helicopter rotors (rotors designed for edgewise flight), but correlation activities for tiltrotors have been limited, in part by the absence of appropriate measured data. The test of the Tilt Rotor Aeroacoustic Model (TRAM) with a single, 0.25-scale V-22 rotor in the German-Dutch Wind Tunnel (DNW) now provides an extensive set of aeroacoustic, performance, and structural loads data.

This report documents correlation between the TRAM DNW measured performance and airloads data and CAMRAD II calculations. CAMRAD II is a modern rotorcraft comprehensive analysis, with advanced models intended for application to tiltrotor aircraft as well as helicopters. Comprehensive analyses have undergone extensive correlation with performance and loads measurements on helicopter rotors. The present paper is part of an initial effort to perform an equally extensive correlation with tiltrotor data. The comparison of measurements and calculations presented here focuses on performance and airloads in hover and helicopter mode operation. The correlation establishes the level of predictive capability achievable with current technology; identifies the limitations of the current aerodynamic and wake models of tiltrotors; and leads to recommendations for research to extend tiltrotor aeromechanics analysis capability.

TRAM DNW Test

The purpose of the Tilt Rotor Aeroacoustic Model (TRAM) experimental project is to provide data necessary to validate tiltrotor performance and aeroacoustic prediction methodologies and to investigate and demonstrate advanced civil tiltrotor technologies.

In April-May 1998 the TRAM was tested in the isolated rotor configuration at the Large Low-speed Facility of the German-Dutch Wind Tunnels (DNW). A preparatory test was conducted in December 1997. These tests were the first comprehensive aeroacoustic tests for a tiltrotor, including not only noise, performance, and structural loads data, but airload and wake measurements as well. The TRAM and the DNW test are described in references 1 to 4. Figure 1 shows the wind tunnel installation of the TRAM isolated rotor. The DNW is a closed return, atmospheric pressure wind tunnel. The TRAM test utilized the 6- by 8-meter open-jet test section, which is in a large anechoic testing hall.

The Tilt Rotor Aeroacoustic Model (TRAM) is a general-purpose test bed for moderate-scale tiltrotor models. TRAM consists of two hardware-interchangeable test rigs: an isolated rotor test stand, and a full-span, dual-rotor model. The contractor team of MicroCraft and McDonnell Douglas

Figure 1. Tilt Rotor Aeroacoustic Model in the German-Dutch Wind Tunnel (TRAM DNW).

Helicopter (now Boeing) had overall responsibility for the TRAM development, under the direction of the Aeromechanics Branch, Army/NASA Rotorcraft Division, NASA Ames Research Center.

TRAM Physical Description

The TRAM was designed as a 0.25-scale V-22 tiltrotor aircraft model. The rotor has a diameter of 9.5 ft. The rotor was tested at a tip Mach number of 0.63 in helicopter mode (because of operational limitations, this was lower than the V-22 nominal tip Mach number of 0.71); and 0.59 in airplane mode (matching the V-22). The rotor and nacelle assembly was attached to an acoustically-treated, isolated rotor test stand through a mechanical pivot (the nacelle conversion axis), as shown in figure 1. The nacelle (but not the spinner) contours model the V-22. The test stand contained the electric motor assembly, and was attached to the DNW sting mount. The conversion angle was manually adjusted, set to 90 deg nacelle angle for helicopter mode and 0 deg nacelle angle for airplane mode testing.

Reference 5 provides complete details of the TRAM physical description. Table 1 presents the principal characteristics of the TRAM. The solidity $\sigma = 0.105$ is the official value (thrust-weighted), used to normalize measured and calculated data in this report. Figure 2 shows the blade chord and twist distributions.

The TRAM blade airfoils are the V-22 airfoils designated XN28, XN18, XN12, XN09, at radial stations r/R = 0.2544, 0.50, 0.75, 1.00 respectively. The root fairing has a special airfoil section. The airfoil tables used in the present investigation are those generated during the JVX program in the mid 1980's. Reference 6 is the source of the airfoil data. The data are from pressure wind tunnel tests of 6.5 inch chord airfoils, at Reynolds number of approximately Re/M = 15 to 20 million (M is the Mach number). For the root fairing the V-22 cuff airfoil data were used, although the contours of the

Table 1. Principal physical characteristics of the TRAM model.

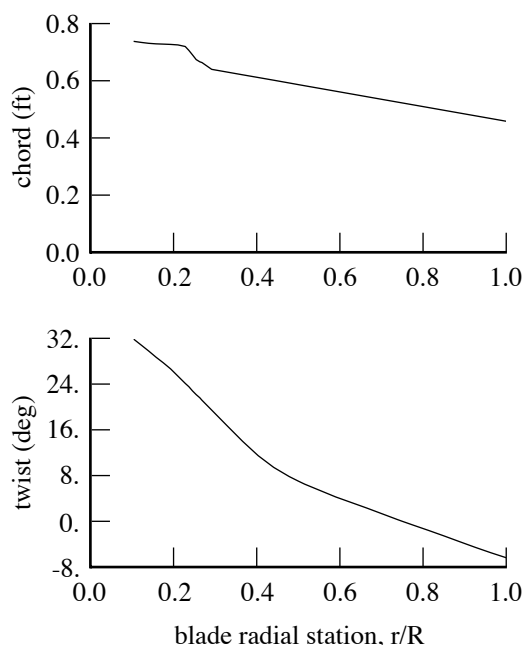| gimballed hub, trailing pitch link	
blade radius R	4.75ft = 1.45m
solidity σ (thrust weighted)	0.105
number of blades	3
100% rpm, helicopter	$M_{tip} = 0.708$
100% rpm, airplane	$M_{tip} = 0.593$
airfoil sections	XN28, XN18, XN12, XN09
precone	2 deg
nominal pitch flap coupling, δ_3	–15 deg

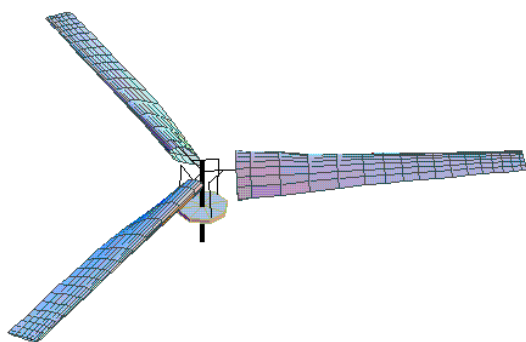Figure 2. TRAM chord and twist distributions.

Figure 3. CAMRAD II model of TRAM.

TRAM root fairing do not match the V-22 because of constraints imposed by the blade pitch case geometry and construction.

The rotor blades and hub are designed as geometrically and dynamically scaled models of the V-22 blades. The hub is gimbaled with a constant velocity joint consisting of a spherical bearing and elastomeric torque links. The balance and flex-coupling measure forces and torque. The blade set has both strain-gauged and pressure-instrumented blades. There are 150 pressure transducers distributed over two right-hand rotor blades: primarily at radial stations 0.50, 0.62, 0.82, and 0.96 on blade #1, and at radial stations 0.33, 0.72, 0.90, and 0.98 on blade #2. At the start of the test, 135 of the pressure gages were operational. These pressure measurements can be integrated chordwise to obtain blade section normal force at seven radial stations (there are too few chordwise points at 98% radius to get section normal force). Reference 3 describes the data reduction process for the blade pressures and section normal force. The third blade carries all of the required safety of flight strain gauge instrumentation.

Rotorcraft Analysis

The TRAM was analyzed using the rotorcraft comprehensive analysis CAMRAD II. CAMRAD II is an aeromechanical analysis of helicopters and rotorcraft that incorporates a combination of advanced technologies, including multibody dynamics, nonlinear finite elements, and rotorcraft aerodynamics. The trim task finds the equilibrium solution (constant or periodic) for a steady state operating condition, in this case a rotor operating in a wind tunnel. For wind tunnel operation, the thrust and flapping (longitudinal and lateral gimbal tilt) are trimmed to target values. The aerodynamic model includes a wake analysis to calculate the rotor nonuniform induced-velocities, using rigid, prescribed or free wake geometry. The results presented here were all obtained using a free wake. CAMRAD II is described in references 7 to 11. CAMRAD II and similar analyses have undergone extensive correlation with performance and loads measurements on helicopter rotors (see, for example, ref. 9). The present paper is part of an initial effort to perform an equally extensive correlation with tiltrotor data.

Figure 3 illustrates the CAMRAD II model of the TRAM. The analytical model has a fixed shaft (no test stand dynamics) and constant rotor rotational speed (no drive train dynamics). The hub has a gimbal joint at the center of rotation, with nominal pitch/gimbal coupling of δ_3 = –15 deg. Additional details of the model are given in reference 12. The CAMRAD II solution for the periodic rotor motion
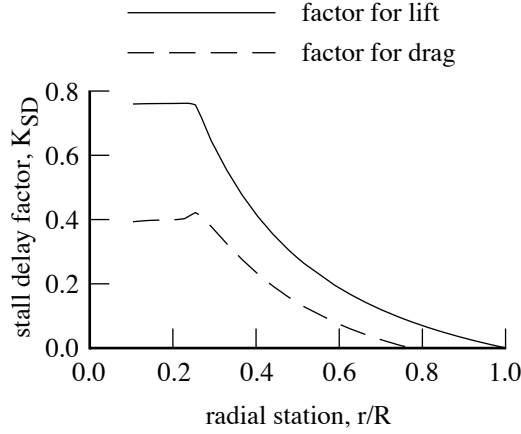
Figure 4. Stall delay factor for TRAM blade.

in trim used 10 harmonics of 12 cantilever elastic blade modes plus the gimbal degree of freedom.

The aerodynamic model uses lifting-line theory with a vortex wake calculation of the induced velocity. The blade aerodynamic surfaces are represented by 16 panels, from the root cutout of r/R = 0.10558 to the tip, with panel widths varying from 0.09R inboard to 0.025R at the tip. Midpoints of seven of the aerodynamic panels are aligned with the pressure instrumentation on the TRAM blades, to avoid additional interpolation in the comparison of calculated and measured airloads. The drag coefficients in the airfoil tables are corrected to the lower Reynolds number of the 0.25-scale model, using a factor equal to the Reynolds number ratio to the 1/5-power.

There is evidence that rotational effects on the boundary layer produce a delay of separation on rotor blades, particularly for the inboard sections of tiltrotors and wind turbines (refs. 13 and 14). This stall delay is modelled using input factors K_{sd} to modify the lift and drag coefficients obtained from the airfoil tables:

$$c_l = c_{l\ table} + K_{sdL}\left(c_{l\alpha}(\alpha - \alpha_z) - c_{l\ table}\right)$$

$$c_d = c_{d\ table} + K_{sdD}\left(c_{dz} - c_{d\ table}\right)$$

where $c_{l\alpha}$ is the lift-curve slope, and α_z and c_{dz} are the angle of attack and drag coefficient at zero lift. The equations given by Selig (ref. 14) are used to evaluate the stall delay factors, which depend on the blade chord distribution. The values of K_{sd} used in the TRAM analysis are shown in figure 4.

The CAMRAD II rotor wake analysis uses second-order lifting line theory, and the general free wake geometry described in references 10 and 11. For helicopter mode operation (edgewise flight at moderate speed, $\mu = 0.125$ to 0.200), the high twist of the tiltrotor blades results in negative tip loading over most of the advancing side. Hence the dual-peak

model must be used, in which the tip vortex is defined by the negative tip loading (not by the maximum positive bound circulation on the inboard part of the blade). A core radius of 20% mean chord is used for the tip vortex. The positive trailed vorticity inboard of the negative tip loading also rolls up in the analysis, with a core radius of 30% mean chord. To avoid having the rollup model respond to small regions of negative loading, the dual-peak model is only used at azimuths where the negative loading extends inboard at least to 0.945R (there are two aerodynamic panels outboard of this radial station). Two revolutions of wake are used, with calculated free distortion. There is partial entrainment of the trailed vorticity into the tip vortex, such that the final tip vortex strength (achieved after 1/4 revolution of wake age) is 70% of the peak bound circulation on the blade. The distorted wake geometry is calculated for the inboard vorticity as well as for the tip vortices, since inboard rollup is used in the negative tip loading areas. However, distortion of the inboard vorticity is not too important, except when drawing the wake geometry. These wake model features and parameters were determined based on the correlation with measured TRAM performance and airloads, as presented below. The resulting wake model is not the same as the model that has been established for helicopter rotors (refs. 10 and 11).

Work with helicopter rotors has established the importance of rolled-up tip vortices in the calculation of the blade airloading. The resulting blade-vortex interactions are dominant contributors to noise, vibration, and oscillatory structural loads in low speed flight. The tiltrotor wake model used in this report also has a rolled-up tip vortex, although with partial entrainment as described above. In addition, airloads calculated using a wake model with multiple trailed vortex elements are presented here. Bruce Charles of The Boeing Company (Mesa) determined that such a wake model gives good correlation with the measured airloads. The multiple-trailer wake model has a discrete trailed vortex line emanating from each of the aerodynamic panel edges. The calculation of the free wake geometry in CAMRAD II includes the distortion of all of these trailed lines.

The calculations were performed for specified advance ratio (V/ΩR), tip Mach number, and shaft angle of attack. The analysis trim loop adjusts collective and cyclic to achieve target values of the rotor thrust (C_T/σ) and mean gimbal tilt. The shaft angle of attack values in the analysis correspond to the measured values with wind tunnel wall corrections applied. For comparison of trends with operating condition, involving many measured points, the target thrust is a nominal value and the

target gimbal tilt is zero. For comparison with specific data points, the measured thrust and measured one per-rev gimbal tilt are the target trim values for the analysis. Similarly, for trends the operating condition is defined by nominal values of advance ratio, tip Mach number, shaft angle of attack, air density, and temperature; while for specific data points the measured values are used.

In the calculations it is possible to separately evaluate the induced power and the profile power. The induced power can be presented as the ratio $\kappa = C_{Pi}/C_{Pideal}$, where C_{Pideal} is the ideal power obtained from momentum theory. The profile power can be presented as an equivalent blade drag coefficient, $c_{do} = 8C_{Po}/\sigma$, although in airplane mode this expression does not account for the effect of high axial velocity on the profile power.

Data Reduction and Corrections

All measured quantities were sampled at 64 per-rev, except for the pressure and acoustic measurements, which were sampled at 2048 per-rev. Data were collected for 64 revolutions. The results in this report are from a single revolution of data obtained by averaging over the 64 revolutions collected. To eliminate high frequency noise, the airloads data are harmonically analyzed, and 64 harmonics are used to reconstruct the time history at 256 points in a revolution (reduced from 1024 harmonics representing 2048 samples). All the blade-vortex interaction events in the section normal force data are captured using 64 harmonics.

The measured balance loads of the TRAM in the DNW are corrected for the influence of the wind tunnel walls, by using the corrected shaft angle of attack and wind axis propulsive force. Reference 12 describes the wind tunnel wall correction in more detail, and shows the influence of this correction on the performance correlation.

Aerodynamic tares are subtracted from the measured rotor forces and torque. For helicopter mode, the blades were removed but the root fairings around the pitch cases were retained; and the ends of the root fairings were sealed with foam inserts. These tare corrections remove the effects of gravity, the spinner, and (for helicopter mode) the blade root fairings from the measured performance data. The calculated performance (forces and power) does not include the blade weight, and the analysis does not model the spinner. The analysis does include the root fairing, so for helicopter mode it is necessary to apply a tare correction to the calculated performance. With these tare corrections, the measured and calculated performance data can be directly compared. The calculations must include the root fairing, since the root fairing does influence the wake and the loading on the rest of the blade. Reference 12 describes the analysis tare correction in more detail, and shows the influence of this correction on the performance correlation.

The data reduction process for the pressure and airloads measurements is described in reference 3. The pressure coefficient is obtained from the pressure by dividing by the local section dynamic pressure: $c_p = p/(\frac{1}{2}\rho U^2)$. It follows that the section normal force coefficient, obtained by integrating the pressure coefficients, is $c_n = N/(\frac{1}{2}\rho U^2 c)$; where c is the local chord. Since the operating conditions of interest in this report do not involve significant stall at the measurement locations, it is more interesting to look at the quantity $M^2 c_n = N/(\frac{1}{2}\rho a^2 c)$, where $M=U/a$ is the section Mach number. The section airloads can be integrated to obtain the rotor thrust. A comparison of the rotor thrust measured by the balance with the rotor thrust obtained by integrating the blade pressure measurements shows that the thrust from the airloads is consistently lower than the thrust from the balance, by 15 to 19%. The balance measurement of rotor thrust is considered accurate. The cause of this difference is not known. Examination of the chordwise pressure distributions at the seven radial stations does not suggest any problem.

DNW Test Results

The operating conditions of the TRAM in the DNW covered helicopter mode, airplane mode, and hover. The rotor shaft angle of attack is positive aft, around zero (–14 to +14 deg) for helicopter mode and around –90 deg for airplane mode. The tip Mach number M_{tip} is the ratio of the rotor tip speed to the speed of sound. The advance ratio μ is the ratio of the tunnel speed to the rotor tip speed, regardless of the shaft angle. The helicopter mode test points are for nominal advance ratios of μ = 0.125, 0.150, 0.175, 0.200; nominal thrust coefficients of C_T = 0.009, 0.011, 0.013; at shaft angles from –14 deg to 12 deg. Hover tests were conducted in both helicopter mode and airplane mode (shaft angle of 0 and –76 deg respectively, with the tunnel circuit 90% blocked for airplane mode), at thrusts up to approximately C_T/σ = 0.17. The airplane mode configuration was anticipated to be better for hover, since blockage from the model support is minimized in this configuration. Reference 12 provides further details of the TRAM test results from the DNW.

Hover Performance

Hover correlation begins with data from the test of a 0.658-scale model of the JVX rotor (an early version of the design that became the V-22). The JVX hover test results are given in reference 15. The rotor radius was 12.5 ft (XV-15 radius). The JVX blades had the same twist, taper, and thickness-to-
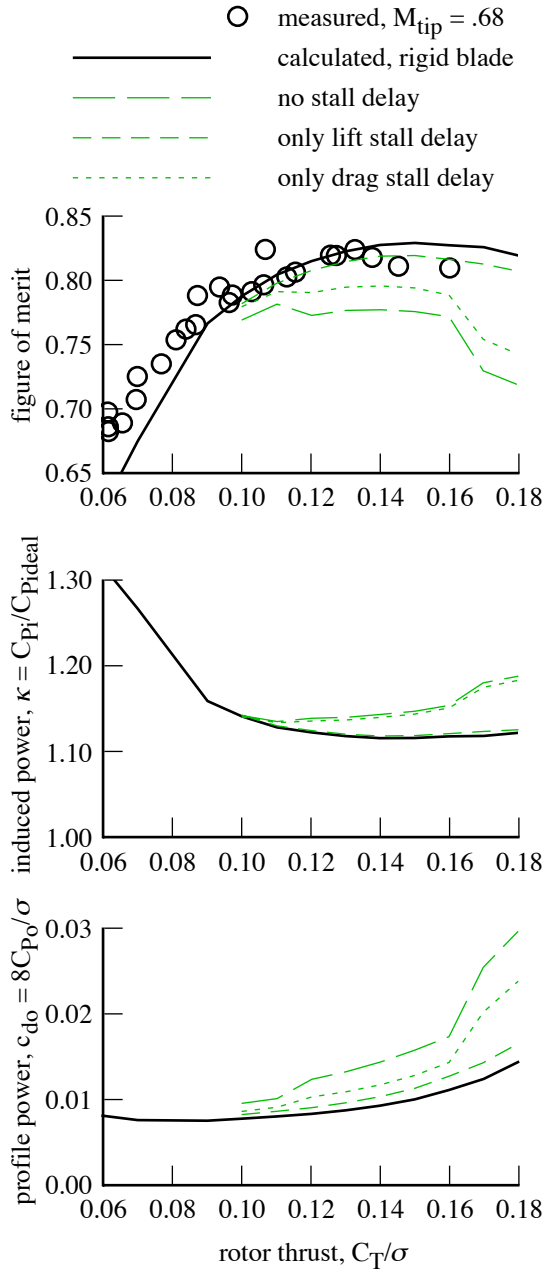
Figure 5. Influence of aerodynamic parameters on calculated JVX hover performance.

Figure 6. Comparison of JVX and TRAM calculated hover performance.

chord ratio as the V-22 blades, but with 8.4% larger chord (solidity of $\sigma = 0.1138$ instead of 0.105). The JVX blades used the XN28, XN18, XN12, XN09 airfoils at radial stations r/R = 0.09, 0.50, 0.75, 1.00 respectively. The JVX blades had a root cutout of about 0.1R, without the cuff of the V-22 and TRAM blades. Hence the JVX chord and twist are similar to the TRAM values shown in figure 2, but with the chord increased by a factor 1.084 and the linear taper extending to the root cutout; and the twist linear from 0.3R inboard to the root cutout. The measured JVX data are for $M_{tip} = 0.68$ and wind speeds below 0.5 m/sec (1 knot); see figure 18a of reference 15.

The measured and calculated JVX hover performance are compared in figure 5. The calculated peak figure of merit matches the measured data well, but the calculated power is too large at the lowest thrust shown, and too small at the highest thrust. Figure 5 shows the influence of the stall delay model on the calculated JVX hover performance. The stall delay has a major influence on the calculated performance. Without the stall delay, the induced power ratio κ is larger at high thrust and the profile power is much larger, with the result that the figure of merit is much too low at moderate and high thrust. The drag stall delay has some influence, but most of the effect is from the lift stall delay. The lift stall delay allows the inboard sections of the blade to produce more lift and thus the outboard sections less lift at a given thrust. This lift redistribution is small, but sufficient to significantly reduce the induced and profile losses at the tip.

Figure 6 compares the calculated hover performance of the JVX and TRAM rotors. The analysis model is changed from the JVX in steps: tip Mach number $M_{tip} = 0.625$; solidity $\sigma = 0.105$ and the TRAM chord; blade cuff chord, quarter-chord locus, and twist; cuff airfoil table; Reynolds number correction; and the TRAM precone, hinge, and stall delay. This last model is the TRAM rotor. The reduction in chord reduces the power, but does not change the figure of merit as a function of C_T/σ
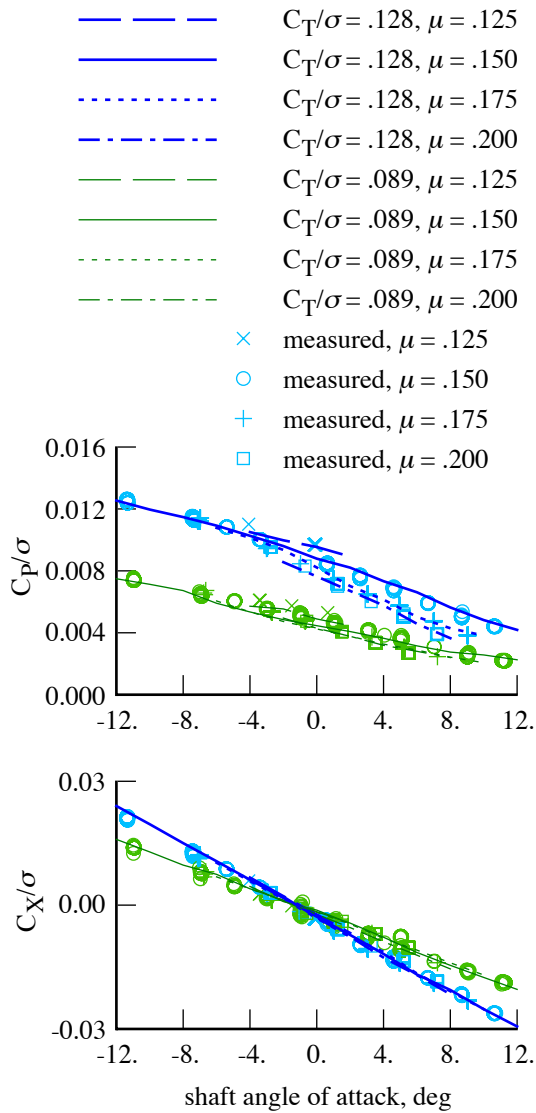
Figure 7. Measured and calculated TRAM helicopter mode performance (rigid blade model).

four advance ratios. Most of the reduction of power as angle of attack increases is accounted for by the parasite power (μC_X), but the equivalent drag still shows a decrease with angle of attack, indicating that the tiltrotor (like the helicopter rotor) becomes more efficient as the propulsive force is reduced. The power increases with thrust, and decreases with advance ratio, as expected at low speed. Most of the variation of the propulsive force with shaft angle of attack and thrust is accounted for by the tilt of the thrust vector with the shaft (αC_T), so the shaft-axis inplane force is a relatively constant drag value. Figure 7 compares the measured helicopter mode performance with calculations using a rigid blade model and the tiltrotor aerodynamic and wake model described above. The calculated power generally matches the measurements well, although the calculated power is too low at low thrust and the middle of the angle of attack range; and the slope with angle of attack is somewhat too small for $\mu = 0.15$ and high thrust. In addition, the calculated power is somewhat erratic, reflecting the complexity of the wake at these operating conditions. The calculated propulsive force matches the data well, so the differences between measurement and calculation are similar for power and equivalent drag. Both the wind tunnel wall correction and the analysis tare correction are required for best correlation between measured and calculated performance (reference 12). There was little influence of the blade elastic motion on the calculated performance.

The influence of the aerodynamic model on the calculated TRAM helicopter mode performance for $\mu = 0.15$ is examined in figure 8. Without the Reynolds number correction of the drag from the airfoil tables, the calculated power is too low. Without the stall delay model, particularly for the lift, the calculated power is much too high, especially at the higher thrust. Without the stall delay model, the equivalent drag actually increases with angle of attack, because of an increase in the stall at the blade root. The stall delay model is required for accurate calculation of the tiltrotor performance in helicopter mode forward flight. Note however that at low thrust and the middle of the angle of attack range, without the stall delay the induced power is higher, perhaps more realistic (reflecting the influence on the wake of the lift distribution changes produced by the stall delay model). This implies that a better stall model is needed.

The influence of the wake model on the calculated TRAM helicopter mode performance for $\mu = 0.15$ is examined in figure 9. The wake model for the baseline uses the dual-peak wake model, to accommodate the negative loading on the advancing tip of the blade in helicopter mode; partial
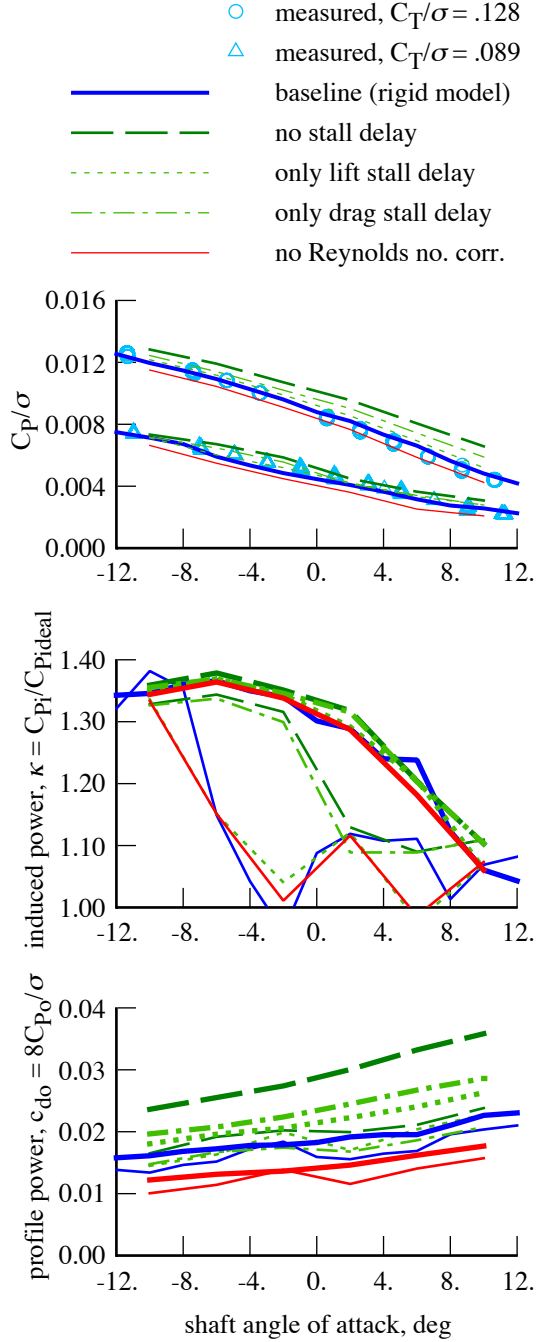
much. The cuff airfoil properties reduce the figure of merit somewhat. The Reynolds number correction significantly increases the power and reduces the figure of merit. Primarily these steps change the profile power. The other steps in figure 6 have little effect. As for the JVX rotor, the calculated peak figure of merit for TRAM matches the data well, but the calculated power is too large at the lowest thrust shown, and too small at the highest thrust; and as for the JVX rotor, the stall delay model (figure 4) can influence the shape of the power and figure of merit as a function of thrust.

Helicopter Mode Performance

The TRAM helicopter mode performance measured in the DNW is shown in figure 7, in terms of rotor power and propulsive force as a function shaft angle of attack for two rotor thrust values and

Figure 8. Influence of aerodynamic model on calculated TRAM helicopter mode performance (μ = 0.15; in lower two figures, heavy line C_T/σ = 0.128, thin line C_T/σ = 0.089).
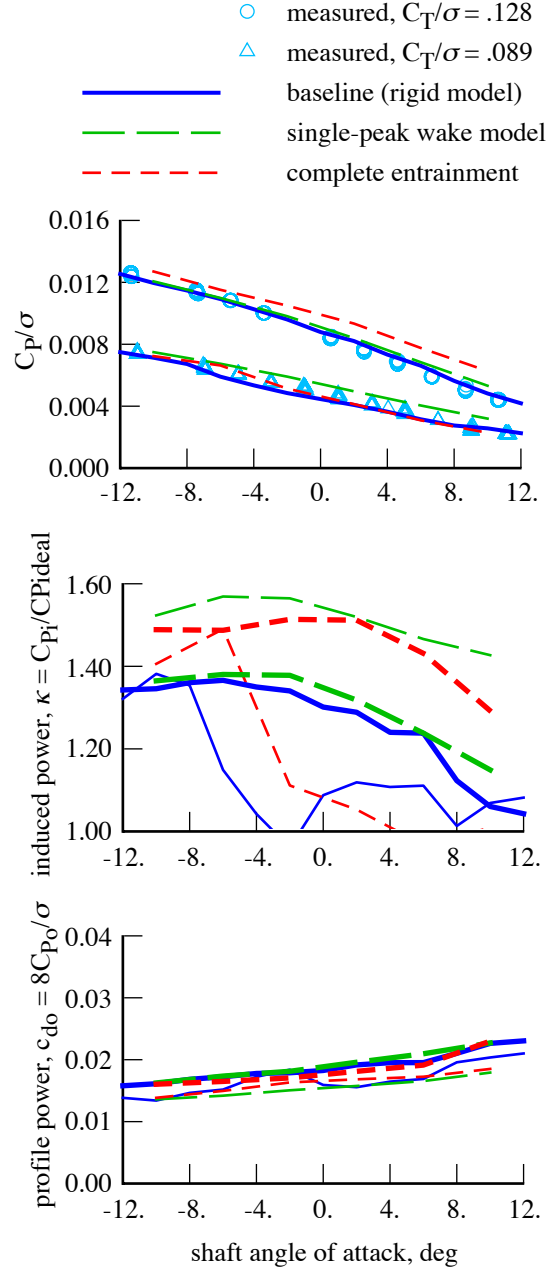
Figure 9. Influence of wake model on calculated TRAM helicopter mode performance (μ = 0.15; in lower two figures, heavy line C_T/σ = 0.128, thin line C_T/σ = 0.089).

entrainment of the trailed vorticity into the tip vortex, such that the final tip vortex strength (achieved after 1/4 revolution of wake age) is 70% of the peak bound circulation on the blade; two revolutions of wake; and a search for the circulation peak only inboard of 0.945R, to avoid having the rollup model respond to small regions of negative loading. Figure 9 shows that using the single-peak wake model increases the calculated power for low

thrust, where there is significant negative loading of the blade tip. Using complete entrainment of the tip vortex increases the calculated power for high thrust. For both of these effects, the source of the power increase is a substantial increase of the induced power. The ratio of the tip vortex strength to the peak bound circulation (70% here) is a fixed parameter in this model. It is likely that this ratio actually varies with azimuth.

Through extensive correlation of CAMRAD II calculations with performance and airloads

Legend:
○ measured, $C_T/\sigma = .128$
△ measured, $C_T/\sigma = .089$
——— tiltrotor model
—·—·— multiple-trailer wake model
– – – helicopter model

(vertical axes, top to bottom: C_P/σ; induced power, $\kappa = C_{Pi}/C_{Pideal}$; profile power, $c_{do} = 8C_{Po}/\sigma$; horizontal axis: shaft angle of attack, deg)
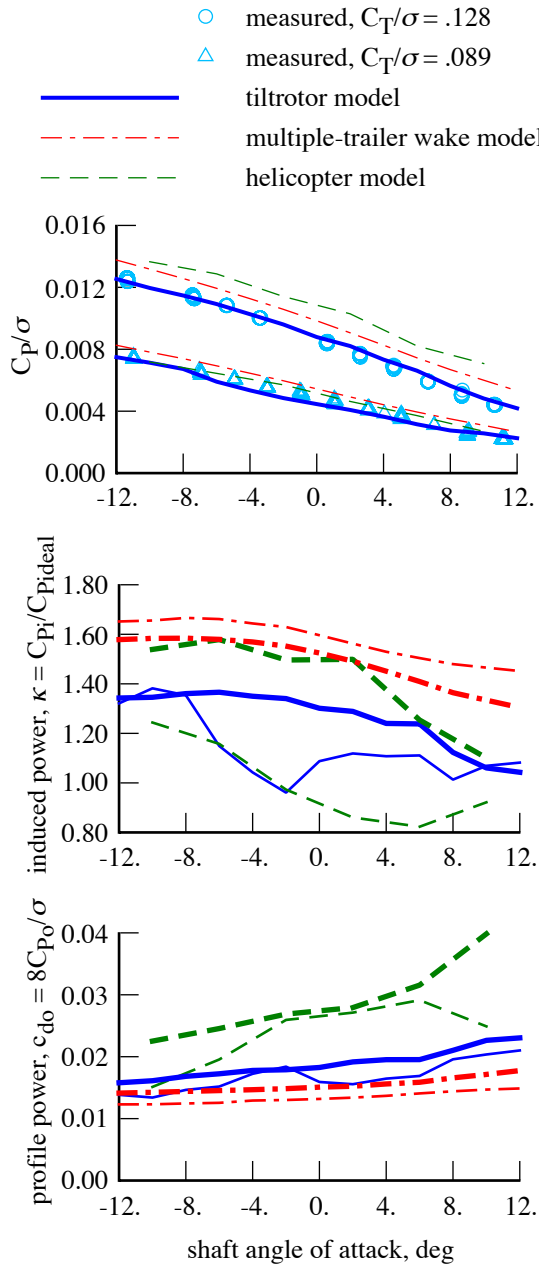
Figure 10. TRAM helicopter mode performance calculated using tiltrotor and helicopter aerodynamic and wake models ($\mu = 0.15$; in lower two figures, heavy line $C_T/\sigma = 0.128$, thin line $C_T/\sigma = 0.089$).

measurements, an aerodynamic and wake model appropriate for most helicopters has been developed (refs. 9 to 11). Figure 10 compares the measured TRAM helicopter mode performance with calculations using this helicopter aerodynamic and wake model, and with calculations using the tiltrotor aerodynamic and wake model documented in this report. The primary differences are that the helicopter model does not include the stall delay, and uses complete entrainment of the tip vortex, three revolutions of wake, and unrestricted search for the circulation peak. For both the tiltrotor and helicopter

models, the dual-peak wake model is used, since there is significant negative loading on the rotor blade. At high thrust, the calculated power is much too large with the helicopter model. This power increase is caused by increases both in profile power (without the stall delay) and in the induced power (with complete rollup), as shown in figure 10. Figure 10 also shows that at low thrust the induced power is unreasonably low with the helicopter model (less than the ideal momentum theory value), while the profile power is increased. So at low thrust, the power calculated using the helicopter model shows good correlation with the measured power only because of canceling errors in the calculated induced and profile power. The span loading and wake formation are very different on tiltrotors and helicopters, so it is essential to use model features specific to tiltrotors in order to adequately predict the behavior. The high twist of the tiltrotor blade generally means that the peak bound circulation is not near the tip, implying a partial rollup of the trailed vorticity into the tip vortex. The delay of stall by rotational effects on the inboard blade sections is an aerodynamic phenomenon that should exist on helicopters as well as on tiltrotors. With the low twist of helicopter blades, the angle of attack is not high enough on the inboard part of the blade for the stall delay to have a significant role in redistributing the lift load over the rotor disk.

Figure 10 also shows the performance calculated using the tiltrotor model with the multiple-trailer wake model. It will be shown below that good correlation with measured airloads is obtained using the multiple-trailer wake model. However, the power calculated using the multiple-trailer wake model is significantly larger than measured and the propulsive force is larger, in contrast to the good correlation obtained using the rolled-up wake model. With the multiple-trailer wake model the calculated profile power is lower and the calculated induced power is significantly higher than with the rolled-up wake model. Figure 10 shows that the erratic behavior exhibited by results from the rolled-up wake model is absent with the multiple-trailer wake model.

Helicopter Mode Airloads

Figures 11 and 12 compare the measured blade airloads ($M^2 c_n$) with the calculations using various models, at advance ratio $\mu = 0.15$, +6 and –6 deg shaft angle, and two radial stations. The results at other shaft angles and other radial stations are similar. The measured airloads show significant blade-vortex interaction at the tip for all these conditions, at both high and low thrust, and at both positive and negative shaft angles. There is a substantial region of negative loading on the advancing blade tip, particularly at low thrust. Each
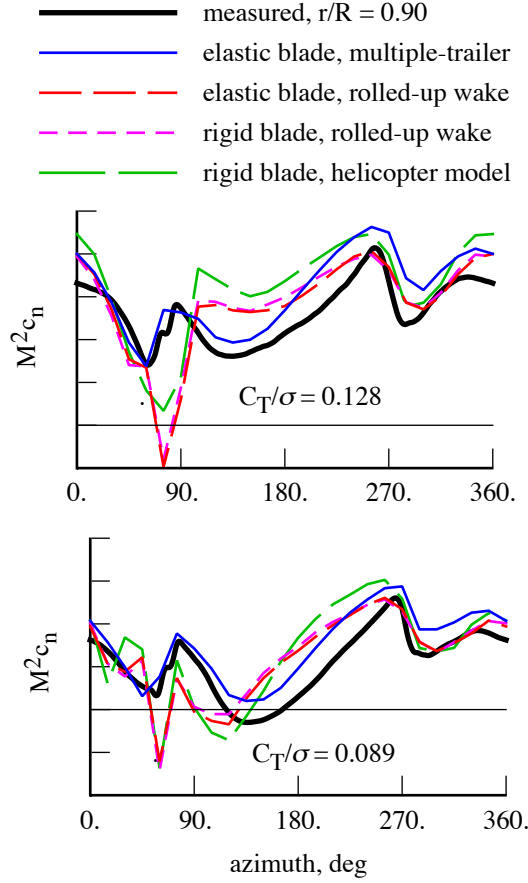
Figure 11. Measured and calculated TRAM helicopter mode airloads for $\mu = 0.15$ and $\alpha_S = -6$, radial station r = 0.90R.

Figure 12. Measured and calculated TRAM helicopter mode airloads for $\mu = 0.15$ and $\alpha_S = 6$, $C_T/\sigma = 0.089$.

figure presents the airloads calculated using the tiltrotor model with elastic blade and multiple-trailer wake; the tiltrotor model with elastic blade and rolled-up wake; the tiltrotor model with rigid blade and rolled-up wake; and the helicopter model with rigid blade. The measured airloads and the airloads calculated using the multiple-trailer wake compare very well. The measured airloads integrate to a smaller rotor thrust, so the calculated airloads tend to have a larger mean value. The airloads calculated using the other wake models differ significantly from the measurements. The calculations using the rolled-up wake model capture the overall character of the airloads, but there are significant differences in the details. There is little influence of the blade elastic motion on the calculated airloads. Compared to the airloads calculated using the tiltrotor aerodynamic and wake model, the helicopter model produces larger blade-vortex interaction amplitude on the retreating side, smaller blade-vortex interaction amplitude on the advancing side for positive shaft angles, and larger peak airloads on the rotor disk.

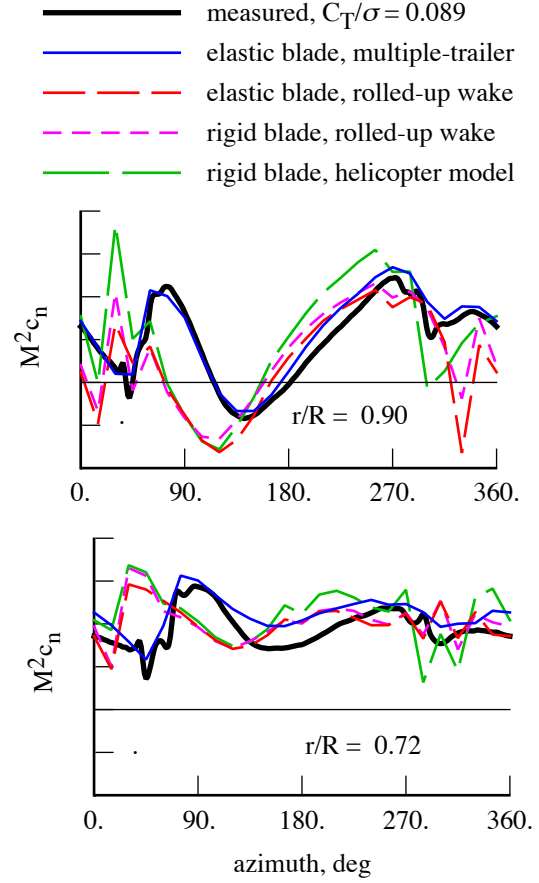Figures 13 and 14 show the calculated wake geometry for +6 and −6 deg shaft angle and low

thrust, with the rolled-up wake model and the multiple-trailer wake model. The vertical lines on the advancing blade (at an azimuth angle of 105 deg) represent the airloading distribution (M^2c_n), with a common scale on all figures. These figures show the substantial wake distortion and blade-vortex interaction on the advancing side (observed for all thrust values and all shaft angles); the negative loading on the advancing tip at low thrust; and the general change in the location of the wake relative to the tip-path plane as the shaft angle is varied from negative to positive (from forward to aft). The overall, large-scale distortion with the multiple-trailer wake model is similar to that with the rolled-up wake model. Entrainment of the outboard lines into a tip vortex is evident, but requires a substantial wake age to develop.

The wake geometry calculated for the multiple-trailer wake exhibits rollup of the outboard lines into a tip vortex, but because of the spanwise resolution and the absence of viscous effects, a highly concentrated tip vortex is not produced. In contrast, measurements of the TRAM flow field show distinct rolled-up vortex structures, including both positive
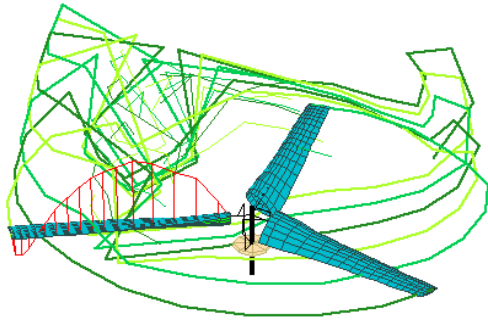
Rolled-up wake model.
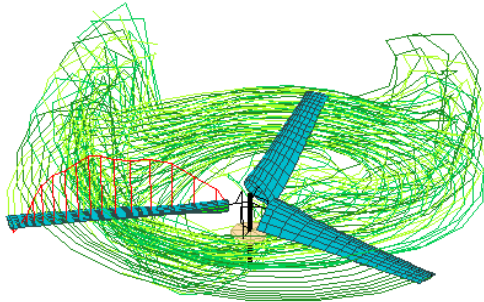
Multiple-trailer wake model

Figure 13. Calculated TRAM wake geometry and loading for $\mu = 0.15$, $\alpha_s = -6$, $C_T/\sigma = 0.089$. Azimuth of reference blade = 105 deg.
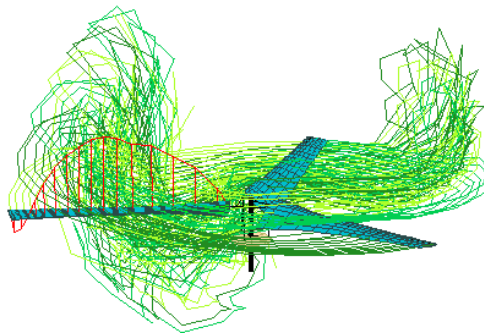

Figure 14. Calculated TRAM wake geometry and loading for $\mu = 0.15$, $\alpha_s = 6$, $C_T/\sigma = 0.089$. Multiple-trailer wake model, azimuth of reference blade = 105 deg.

and negative vortices at low thrust (ref. 16). The vortices produce high-frequency oscillations in the measured airloads (figures 11 and 12), that this multiple-trailer wake model can never produce. In addition, the induced power is larger with the multiple-trailer model, so the performance correlation is not as good as with the rolled-up wake model. It is concluded from these results that while the tiltrotor wake does roll up into concentrated vortices, the rollup process is occurring over a wake age of several revolutions.

Conclusions

Comparisons of measured and calculated aerodynamic behavior of a tiltrotor model have been presented. The measured data are from the test of the Tilt Rotor Aeroacoustic Model (TRAM) with a single, 0.25-scale V-22 rotor in the German-Dutch Wind Tunnel (DNW). The calculations were performed using the rotorcraft comprehensive analysis CAMRAD II. An aerodynamic and wake model and calculation procedure that reflects the unique geometry and phenomena of tiltrotors has been developed. There are major differences between this model and the corresponding aerodynamic and wake model that has been established for helicopter rotors. The primary differences are that the tiltrotor model includes the stall delay, does not use complete entrainment of the tip vortex, uses two revolutions of wake, and uses a restricted search for the circulation peak. Using this tiltrotor model, good correlation has been shown between measured and calculated performance and airloads in helicopter mode.

In hover, the important model features are the stall delay, the wake extent, the initial span station of the tip vortex formation, and the Reynolds number correction. As observed in other investigations, without the stall delay, the induced power is larger at high thrust and the profile power is much larger, with the result that the figure of merit is much too low at moderate and high thrust.

For computation of performance in helicopter mode, important model features are the stall delay, the Reynolds number correction, the dual-peak wake model with restricted search for the circulation peak, the wake extent, and the tip vortex formation. Good correlation of measured and calculated performance is achieved, when the wind tunnel wall correction of the measurements and an analysis tare correction are used. The helicopter aerodynamic and wake model does not give adequate performance calculations. The measured airloads and the airloads calculated using the multiple-trailer wake compare very well. However, the multiple-trailer wake does not produce the rolled-up vortex structures observed in the TRAM flow field measurements and implied by the

measured high frequency airload variations. In addition, the induced power is larger with the multiple-trailer model, so the performance correlation is not as good as with the rolled-up wake model. The good airloads correlation using the multiple-trailer wake model implies that while the tiltrotor wake does roll up into concentrated vortices, the rollup process is occurring over a wake age of several revolutions.

Two aspects of the analysis that clearly need improvement are the stall delay model and the trailed vortex formation model. These features represent specific physical aspects of rotor aerodynamics, that are described directly, but quite simply, in the aerodynamic and wake model of the analysis. One result of the correlation is to establish values of the parameters that define these features in CAMRAD II. The more general results of the correlation are to establish the key importance of these features for tiltrotor aeromechanics behavior, and the need for improved models. A first-principles solution for rotor aerodynamics is the long term goal. Until that is available, more accurate and more general models of the stall delay and the trailed vortex formation are needed. Acquisition of additional detailed aerodynamic measurements will be needed to support such model development.

Acknowledgments

References

1) Young, L.A. "Tilt Rotor Aeroacoustic Model (TRAM): A New Rotorcraft Research Facility." Heli Japan 98: AHS International Meeting on Advanced Rotorcraft Technology and Disaster Relief, Nagarafukumitsu, Gifu, Japan, April 1998.

2) Young, L.A.; Booth, E.R., Jr.; Yamauchi, G.K.; Botha, G.; and Dawson, S. "Overview of the Testing of a Small–Scale Proprotor." AHS International 55th Annual Forum Proceedings, Montreal, Canada, May 1999.

3) Swanson, S.M.; McCluer, M.S.; Yamauchi, G.K.; and Swanson, A.A. "Airloads Measurements from a 1/4–Scale Tiltrotor Wind Tunnel Test." 25th European Rotorcraft Forum, Rome, Italy, September 1999.

4) Johnson, J.L., and Young, L.A. "Tilt Rotor Aeroacoustic Model Project." Confederation of European Aerospace Societies (CEAS), Forum on Aeroacoustics of Rotorcraft and Propellers, Rome, Italy, June 1999.

5) Ames Research Center. "TRAM Physical Description." NASA Report (to be published).

6) Jenks, M.D., and Narramore, J.C. "Final Report for the 2–D Test of the Model 901 Rotor and Wing Airfoils (BSWT 592)." Boeing Report D901–99065–1, June 1984.

7) Johnson, W. "CAMRAD II, Comprehensive Analytical Model of Rotorcraft Aerodynamics and Dynamics." Johnson Aeronautics, Palo Alto, California, 1992–1999.

8) Johnson, W. "Technology Drivers in the Development of CAMRAD II." American Helicopter Society Aeromechanics Specialists Conference, San Francisco, California, January 1994.

9) Johnson, W. "Rotorcraft Aeromechanics Applications of a Comprehensive Analysis." Heli Japan 98: AHS International Meeting on Advanced Rotorcraft Technology and Disaster Relief, Nagarafukumitsu, Gifu, Japan, April 1998.

10) Johnson, W. "A General Free Wake Geometry Calculation for Wings and Rotors." American Helicopter Society 51st Annual Forum Proceedings, Fort Worth, Texas, May 1995.

11) Johnson, W. "Rotorcraft Aerodynamics Models for a Comprehensive Analysis." AHS International 54th Annual Forum Proceedings, Washington, D.C., May 1998.

12) Johnson, W. "Calculation of Tilt Rotor Aeroacoustic Model (TRAM DNW) Performance, Airloads, and Structural Loads." American Helicopter Society Aeromechanics Specialists' Meeting, Atlanta, Georgia, November 2000.

13) Corrigan, J.J., and Schillings, J.J. "Empirical Model for Stall Delay Due to Rotation." American Helicopter Society Aeromechanics Specialists Conference, San Francisco, California, January 1994.

14) Du, Z., and Selig, M.S. "A 3–D Stall–Delay Model for Horizontal Axis Wind Turbine Performance Prediction." AIAA Paper 98–0021, January 1998.

15) Yamauchi, G.K.; Burley, C.L.; Mercker, E.; Pengel, K; and JanakiRam, R. "Flow Measurements of an Isolated Model Tilt Rotor." AHS International 55th Annual Forum Proceedings, Montreal, Canada, May 1999.

16) Felker, F.F.; Signor, D.B.; Young, L.A.; and Betzina, M.D. "Performance and Loads Data From a Hover Test of a 0.658-Scale V-22 Rotor and Wing." NASA TM 89419, April 1987.